Synthesis, Biological Evaluation, and Three-Dimensional Quantitative Structure−Activity Relationship Study of Small-Molecule Positive Modulators of Adrenomedullin

Mario A. García,[†] Sonsoles Martín-Santamaría,[†] Mónica Cacho,[†,‡] Fernando Moreno de la Llave,[†] Miguel Julián,[†] Alfredo Martínez,[§] Beatriz de Pascual-Teresa,*[,†] and Ana Ramos*[,†]

Departamento de Química, Facultad de Farmacia, Universidad San Pablo CEU, Urbanización Montepríncipe, 28668 Boadilla del Monte, Madrid, Spain, and Departamento de Neuroanatomía y Biología Celular, Instituto Cajal, Av. Doctor Arce, 37, 28002 Madrid, Spain

Received January 10, 2005

Adrenomedullin (AM) is a peptide hormone implicated in blood pressure regulation and in the pathophysiology of several diseases such as hypertension, cancer, diabetes, and renal disorders, becoming an interesting new target for the development of drugs. In a recent high-throughput screening study, a positive modulator with a bistriazole structure has been identified.[1] In this work, a new series of structurally related compounds has been synthesized by reaction of phenoxyacetic acid with the corresponding dihydrazide, followed by treatment of the formed bisoxadiazoles with benzylamine. The affinity toward AM of the lead compound, and a structurally related family obtained from the small-molecule NCI library together with the synthesized series, has been determined. A three-dimensional quantitative structure−activity relationship (3D-QSAR) study and conformational and molecular dynamics simulations have shown that the presence of a free NH and a phenyl group is essential for the interaction of these compounds with AM.

Introduction

Adrenomedullin (AM) is a 52 amino acid peptide that belongs to the calcitonin/calcitonin gene-related peptide (CGRP)/amylin/AM superfamily and was isolated in 1993 from a human pheochromocytoma (adrenal tumor).[2] In humans, it is expressed by many cell types and exerts a variety of physiological roles, including vasodilatation, bronchodilatation, hormone regulation, antimicrobial activity, and growth regulation.[3,4] Extensive reviews have recently been published that summarize the state of the art in our collective knowledge on AM science.[5]

AM levels are dysregulated in many human pathologies such as hypertension, heart failure, sepsis, cancer, and diabetes.[4] Several studies have demonstrated that changes in AM levels have opposite effects depending on the particular disease studied. Thus, while AM is a protective agent against cardiovascular disorders,[6] it behaves as a stimulating factor in other pathologies such as cancer[7] and diabetes.[8] Therefore, AM is a new and promising target in the development of molecules that, through their ability to positively or negatively regulate AM activity, could be used in the treatment of these pathologies.

The only attempt in this area has been carried out recently by Martínez et al.[1] This article describes a new and efficient method to detect nonpeptidic modulators of AM from a large library of small molecules that the NCI has collected since 1955. The first phase involves a screening to search compounds that inhibit the binding between AM and its monoclonal antibody. All the compounds that gave a positive response to this assay were subjected to a secondary screening that consisted of an analysis of their ability to modify the production of cAMP, a second messenger elicited by the specific receptor system. This assay allowed classifying the molecules in positive or negative modulators, depending on their ability to elevate or reduce cAMP levels, respectively.

Further assays characterized the physiological impact of selected small molecules in AM-mediated responses. Validation of the biological activity of those compounds was carried out, both as potential antiproliferative agents for the negative modulators and as hypotensive agents for the positive modulators.[1]

Results and Discussion

One of the positive modulators that showed promising behavior by both screening steps mentioned above was bistriazole **1a**. Structurally related chemical family members such as **1b**−**i** were also evaluated, and in most cases they maintained the activity or even showed stronger activity (**1h**) than the lead compound. In this work the synthesis of analogues **1j**−**n** and the study of the structure−activity relationship using computational techniques of compounds **1a**−**n** have been carried out, with the aim of determining the structural requirements for efficient interaction with AM.

Chemistry. The synthesis of bistriazoles **1j**−**n** was carried out following the route outlined in Scheme 1. Thus, phenoxyacetic acid was treated with the corre-

* To whom the correspondence should be addressed. For B.d.P.-T.: phone, 34913724796; fax, 34913510475; e-mail, bpaster@ceu.es. For A.R.: phone, 34913724782; fax, 34913510475; e-mail, aramgon@ceu.es.
[†] Universidad San Pablo CEU.
[‡] Current address: Instituto de Química Médica, C/ Juan de la Cierva, 3, 28006 Madrid, Spain.
[§] Instituto Cajal.

10.1021/jm050021+ CCC: $30.25
Published on Web 05/24/2005

Scheme 1. Synthesis of Series **2**, **3**, and **1j**−**n**[a]

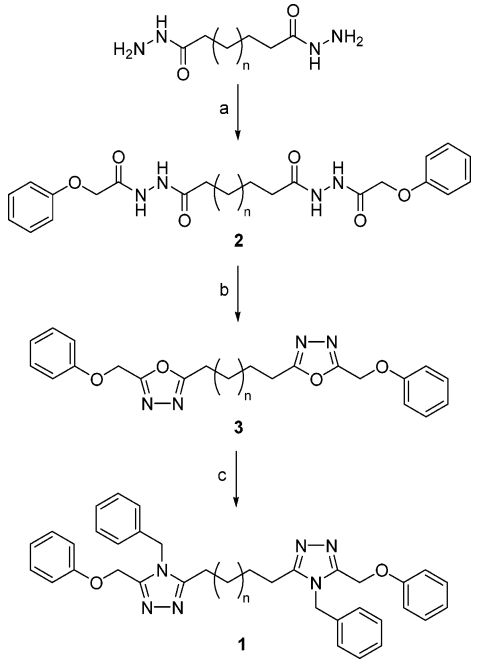

[a] Reagents: (a) (i) phenoxyacetic acid and $POCl_3$ in CH_3CN, Δ; (ii) concentrated NH_3; (b) (i) $POCl_3$ in CH_3CN, Δ; (ii) concentrated NH_3; (c) $PhCH_2NH_2$, Δ.

sponding commercially available dihydrazides in the presence of $POCl_3$ to yield compounds **2j**−**n**. Further refluxing of these with $POCl_3$ in CH_3CN for 7 h brought about the formation of bisoxadiazoles **3j**−**n**. Attempts to undergo the reaction in one step, following the reaction conditions described by Kudari et al.[9] for the synthesis of bisisoxazoles (series **3**) and other analogue compounds, led to the isolation of the open-chain bishydrazides. Finally, reaction of bisoxadiazoles **3j**−**n** with benzylamine yielded the desired bistriazoles **1j**−**n**.

Biological Activity. The affinity of the different compounds for AM was quantified by measuring the interference of the compounds in the binding between the peptide and its blocking monoclonal antibody. A neutralizing monoclonal antibody will bind to an epitope on the peptide that is critical for receptor recognition. Thus, molecules that disrupt peptide−antibody binding may be good candidates as modulators of peptide physiology. Internal controls were placed in every plate as described in Experimental Section (wells without any coating, wells where no potential modulators were added, and wells with a positive inhibition control). The affinity was quantified by comparison with the internal controls (Table 1).

Seven compounds (**1a**,**c**−**h**), all of them bearing an NH group, significantly inhibited binding of the antibody, suggesting a high degree of affinity for AM. However, compounds **1j**−**n**, where the NH group has been replaced by a methylene group, significantly decreased their AM affinity when compared to compounds with an NH group. In addition, all synthetic intermediates (**2** and **3**) were tested and showed poor affinity values.

Table 1. Positive Modulators of AM[a]

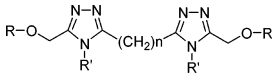

Series 1

compd	*n*	R	R'	% Affinity
1a	8	Ph	NH-Ph	81
1b	8	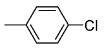	NH_2	19
1c	8	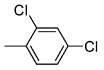	NH_2	48
1d	8	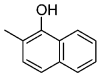	NH_2	42
1e	8	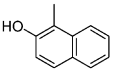	NH_2	46
1f	8	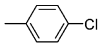	NH-Ph	51
1g	8	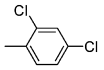	NH-Ph	68
1h	8	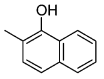	NH-Ph	83
1i	8	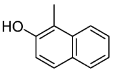	NH-Ph	24
1j	4	Ph	CH_2Ph	19
1k	5	Ph	CH_2Ph	14
1l	6	Ph	CH_2Ph	3
1m	7	Ph	CH_2Ph	20
1n	8	Ph	CH_2Ph	4

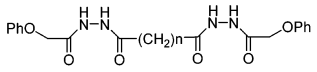

Series 2

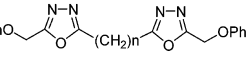

Series 3

compd	*n*	% Affinity	compd	*n*	% Affinity
2j	4	1	**3j**	4	18
2k	5	16	**3k**	5	4
2l	6	20	**3l**	6	10
2m	7	7	**3m**	7	6
2n	8	25	**3n**	8	5

[a] See Experimental Section for compounds **1j**−**n**, **2**, and **3**. Compounds **1a**−**i** belong to the NCI's small-molecule repository.

QSAR Analysis. In cases such as this, in which the target receptor structure is not available, structure−activity relationship (SAR) analysis can often help to elucidate the essential requirements of a potential ligand to interact favorably with its target and indirectly to provide insight into the features that describe the binding site. In this study, a three-dimensional quantitative structure−activity relationship (3D-QSAR) model has been derived for a series of AM ligands, utilizing molecular interaction fields (MIF) calculated in the well-known methodology GRID[10] and the subsequent analysis of these fields by use of alignment-independent descriptors in ALMOND.[11] MIF identify regions where

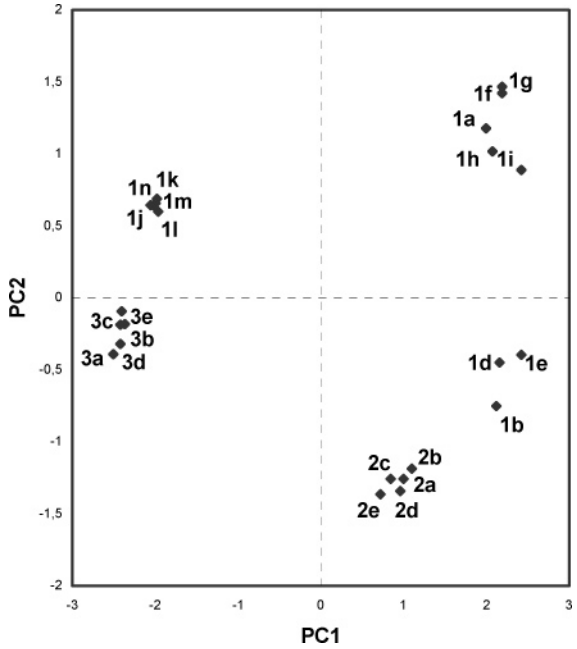

Figure 1. Score plot (which shows the pattern of compounds) of the first (PC1) and the second (PC2) principal components for the 3D-QSAR model.

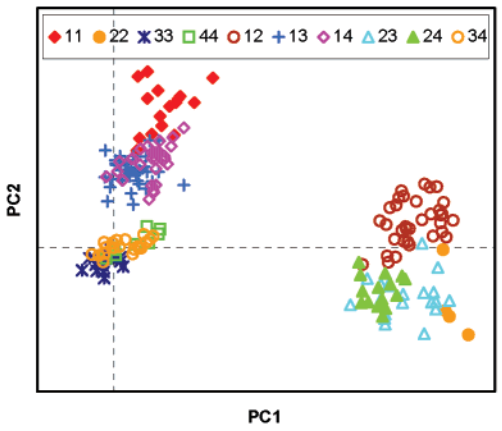

Figure 2. Loading plot (which shows the pattern of descriptors) of the first (PC1) and the second (PC2) principal components for the 3D-QSAR model. Energy descriptors are colored: (11) DRY−DRY; (22) O−O; (33) N1−N1; (44) TIP−TIP; (12) DRY−O; (13) DRY−N1; (14) DRY−TIP; (23) O−N1; (24) O−TIP; (34) N1−TIP.

the ligand can interact favorably with certain chemical groups of a potential receptor, defining a "virtual receptor site" (VRS).[12] On one hand, this approach can assist in the knowledge of the chemical aspects required to bind AM and in the further design of more potent analogues. On the other hand, it can contribute to the scrutiny of the anchoring points that compose the binding site.

The chosen probes were DRY, N1, and O to represent important groups of the peptide AM. The DRY probe represents hydrophobic interactions, the O probe (carbonyl oxygen) represents hydrogen bond acceptor groups, and the N1 probe (amide nitrogen) represents hydrogen bond donor groups. Shape complementarity was also integrated by means of the molecular shape field (TIP "probe"). The compounds show three types of chemical modifications: the length of the aliphatic chain linking the rings (series **1j**−**n**, **2**, and **3**), the nature of the ring (1,3,4-oxadiazole or 1,2,4-triazole), and the substituents R and R′ (Table 1). Compounds **2** and **3** were obtained as intermediates in the synthesis of compounds **1j**−**n** and were also included in the model. Ten correlograms of 92 variables each were obtained, thus producing a matrix of 920 variables and 23 objects.

The model was able to highlight the structural differences between the compounds as is shown in the principal component analysis (PCA) (Figure 1) where compounds are grouped by their chemical structure. The first and second principal components (PCs) explained 96% of the variance of the original descriptors. The first PC extracted, with major contributions from GRIND variables involving the carbonyl oxygen O probe (O−O, DRY−O, O−N1, and O-TIP (Figure 2)), clearly distinguishes the compounds bearing the NH group (series **1**) from the others (series **2** and **3**). This can be rationalized in terms of the strong interactions that NH groups can establish with the O probe. The second PC, which is mostly made up by the GRIND variables involving the hydrophobic DRY probe, is able to separate compounds belonging to the different series in tight clusters. Furthermore, series **1a**−**i** is split into two groups: compounds with R′ = NHPh (**1a**, **1f**, **1g**, **1h**, and **1i**) with high affinity with the exception of **1i**; compounds with R′ = NH_2 (**1b**, **1d**, and **1e**) with moderate affinity. Compound **1c** was not considered at this point to be used later as external set.

The partial least squares (PLS) analysis of the original matrix resulted in a three-component model with an r^2 of 0.93. The cross-validation of the model produced a small positive q^2 value (q^2 = 0.41). A preliminary inspection of the plot representing predicted vs experimental affinities allowed us to identify compound **1i** as an outlier. With the exclusion of compound **1i**, the PLS that was performed on the 22 objects matrix produced a good predictive model, with an r^2 of 0.97 and a cross-validated q^2 of 0.81, for four PCs. Inclusion and exclusion of series **2** and **3** in the model were carefully studied. The predictive ability of the model was slightly improved when considering the whole data, showing that the enrichment in chemical information was relevant to the predictive quality of the model. To simplify the interpretation of the model, the auto- and cross-correlograms that showed low contribution were removed. After the removal of these correlograms, the model contained O−O, DRY−O, O−N1, and O−TIP correlograms, producing a matrix of 368 variables. The PLS of this matrix produced a model of four PCs (r^2 = 0.95, q^2 = 0.84, q^2_{LOO} = 0.87). The model was externally evaluated with compound **1c** (Table 1). The predicted affinity values were very similar to the experimentally measured ones. Figure 3 shows a scatter plot of the calculated vs experimental affinities, including also the affinity prediction.

The inspection of the PLS coefficients showed that all the interactions were positively correlated with affinity (Figure 4). To interpret these results, the correlograms were studied. The O−O autocorrelogram clearly shows that the intensity of the interaction is correlated with the affinity (Figure 5). The variables represent pairs of nodes at different distances where the O probe has favorably interacted. The greatest interactions (red and pink colors, Figure 5) were exhibited by compounds belonging to series **1a**−**i**, which hold a free NH group

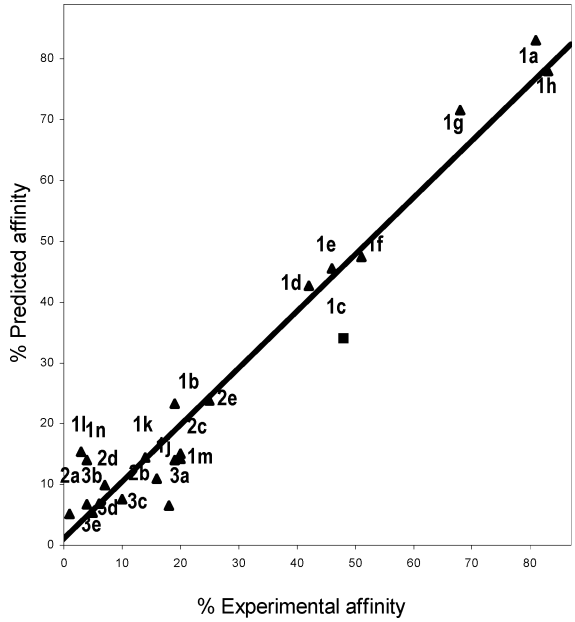

Figure 3. Plot of recalculated versus experimental affinities in the 3D-QSAR model, showing the prediction for compound **1c** (■).

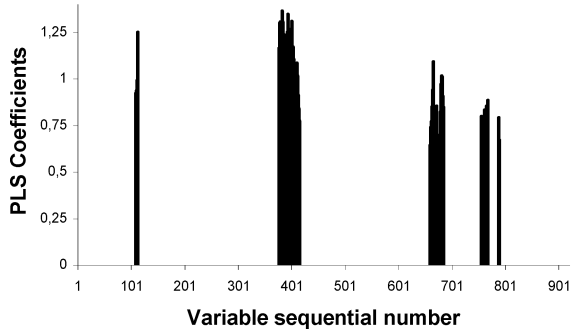

Figure 4. PLS pseudocoefficients histogram for the 3D-QSAR model represented.

that might act as hydrogen bond donor in the interaction with the receptor. Effectively, compounds **1a**−**i** showed an interaction defined by a pair of nodes between both NH groups. Thus, compounds such **1n**, which could be considered as a potential bioisoster of the lead compound **1a**, did not show significant affinity. This finding might suggest that for this family of compounds the NH group is a relevant group for the binding to AM through formation of a hydrogen bond with a residue of the binding pocket.

Other interactions that were shown to be important were those involving DRY probe (DRY−O correlogram) and the molecular shape field (O−TIP correlogram). The MIF corresponding to those nodes coincided around the substituents of type R (Figure 6). This result could indicate that the presence of aromatic rings, which establish van der Waals interactions with the receptor, is favorable for the binding and, furthermore, that those rings must have suitable convexity and shape. Compounds **1a**, **1g**, and **1h**, which presented the highest affinity, also exhibited intense interactions with DRY and TIP probes surrounding the phenyl at the NH group. This could highlight the presence of a secondary hydrophobic pocket, not essential for AM binding but that could be playing a relevant role in order to enhance the affinity toward AM.

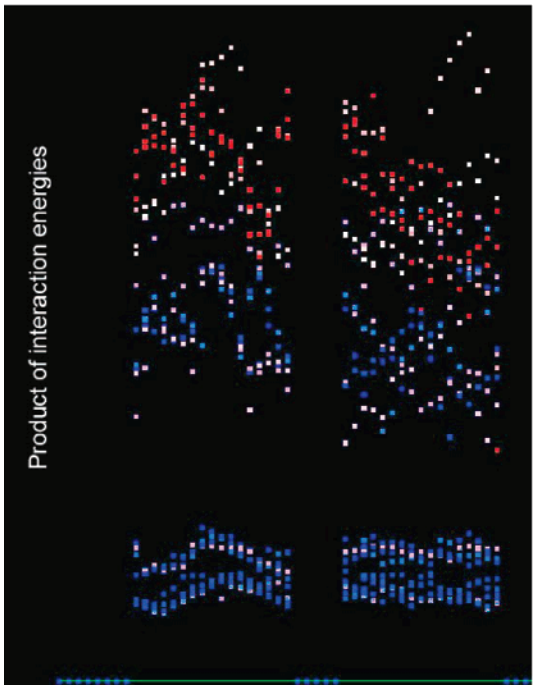

Figure 5. Set of 23 superimposed correlograms, corresponding to the DRY−O correlogram, representing interactions for ligand hydrogen bond donor and hydrophobic regions. Every point in the correlogram represents the product of two particular nodes for a certain compound. Points are color-coded according to the biological activity of the corresponding compounds; active compounds are in red, intermediate in white, and inactive in blue. A simple visual inspection shows that the strength of the interaction is positively correlated with the biological affinity.

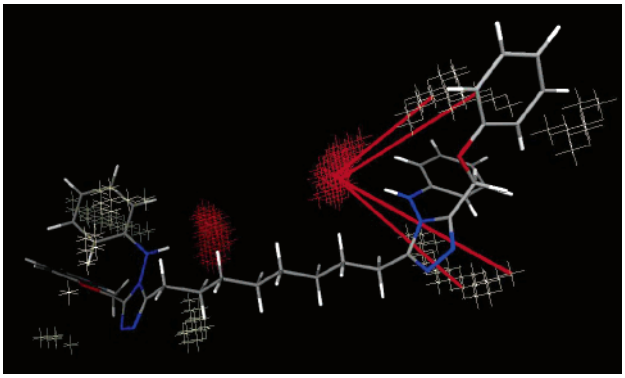

Figure 6. Interactions present in compound **1a**. The fields represent interactions of the probe DRY (white) and O (red).

Conformational and Molecular Dynamics Studies of Compounds 1h and 1i. Despite the structural similarity with **1h**, compound **1i** showed a low affinity value for AM and behaved as an outlier in the QSAR analysis. On the other hand, the other naphthol isomers **1d** and **1e** did not exhibit different behavior as AM modulators, and the QSAR model was able to fit them adequately. It is worth emphasizing that while **1h** and **1i** bear a NH substituted by a phenyl group, **1d** and **1e** have a free NH_2, so the rotational freedom is higher and there is no steric hindrance. To rationalize the different affinity shown by isomers **1h** and **1i**, a thorough conformational study was carried out.

First, a Monte Carlo based conformational search was carried out on the four naphthol derivatives (**1d**, **1e**, **1h**, and **1i**), using the program MacroModel 7.2.[13] Of 1000

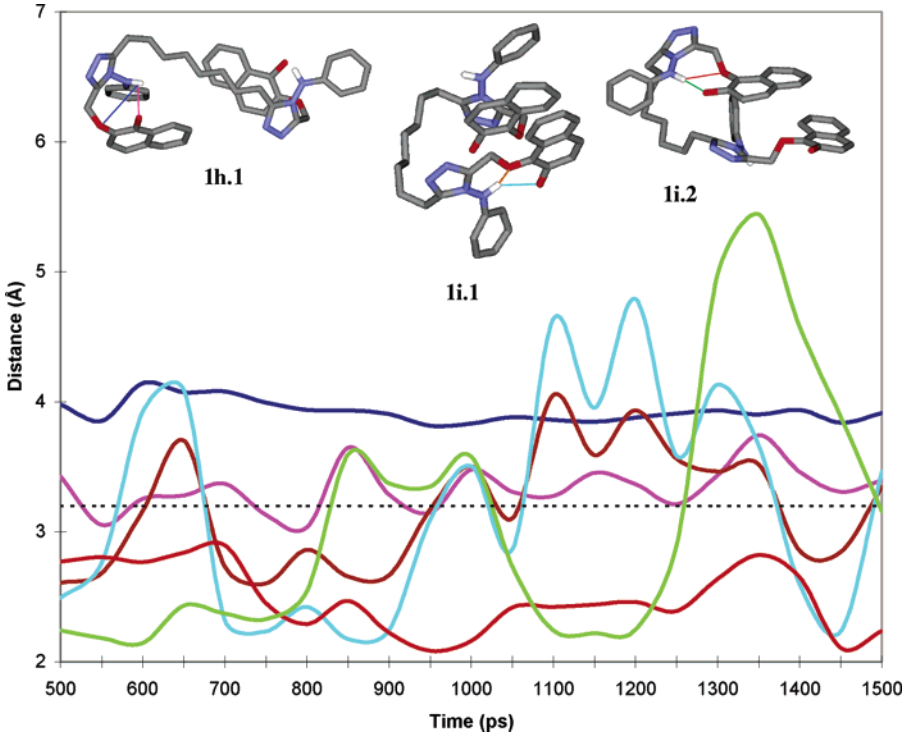

Figure 7. MD trajectories of conformers **1h.1**, **1i.1**, and **1i.2**: NH···O(naphthol) and NH···O(ether) distances. Allowed maximum H···acceptor distance (3.20 Å) is represented as a dotted line.

Monte Carlo pushes of compounds **1h** and **1i**, 454 and 71 unique conformations were found, respectively, within an energetic range of 67−79 kcal mol^{-1} for **1h** and 87−99 kcal mol^{-1} for **1i**. The five energetically lowest conformations for both isomers were inspected, and all possible intramolecular bonds were examined by means of monitoring the distances between oxygen and nitrogen atoms and between polar hydrogens. For every conformer of compound **1i**, eight intramolecular hydrogen bonds were observed, while each conformer of compound **1h** presented only two hydrogen bonds. In many of these bonds, the NH group, whose relevance to the rationalization of the affinity was shown by the 3D-QSAR, was involved as hydrogen bond donor. The conformational search on the other naphthol derivatives, **1d** and **1e**, did not show any important differences (data not shown) between both isomers, as expected.

The stability of the NH−acceptor interactions was checked by performing unrestrained molecular dynamics (MD) simulations in water for compounds **1h** and **1i**, using the AMBER program.[14] The initial geometries were the energetically lowest conformations, and the following ones were under 1.5% of the energetic minimum value. This criterion led to the selection of the lowest energy conformation for compound **1h** (**1h.1**) and two conformers for **1i**, the lowest energy conformer (**1i.1**) and the conformer **1i.2**, which was 0.13 kcal mol^{-1} higher than **1i.1**. Bond distances and angles, where oxygen, nitrogen, and polar hydrogen atoms are involved, were monitored. Figure 7 shows selected results for bonds involving NH hydrogens. The study of these data revealed that **1h.1** holds a stable intramolecular hydrogen bond along the trajectory of the MD simulation between the hydroxyl group and the neighboring ether oxygen. However, NH hydrogen did not take part in any stable bond involving hydroxyl oxygen or ether oxygen (magenta color, Figure 7). The other atoms studied did not exhibit bond distance and angle values corresponding to intramolecular hydrogen bonds. On the contrary, both **1i** conformers presented several intramolecular bonds, with those involving NH hydrogens being of special interest. One of the NH presented bonds to hydroxyl oxygen or ether oxygen or both during most of the MD simulation (Figure 7, **1i.1** conformer, brown and cyan colors; Figure 7, **1i.2** conformer, green and red colors). Bond angle values were in agreement with stable hydrogen bond geometries.

These findings reveal that compound **1i** presents intramolecular bonds involving atoms that are necessary to establish interactions with AM, as NH hydrogen. Accordingly, these interactions might prevent NH from being available to interact with the receptor and would explain the different affinity between **1.h** and **1.i**. Also, these results would be in agreement with the 3D-QSAR analysis, which pointed out the relevance of a free NH to interact with the receptor.

Conclusions

The synthesis, biological evaluation, and 3D-QSAR analysis of a series of positive modulators of AM have been carried out. This research has allowed us to figure out some key aspects of the structural requirements to bind AM, a new and promising target for the development of new molecules with several pharmacological activities. In this particular case, the derived 3D-QSAR model has been able to predict the affinity with a high predictive quality ($q^2_{LOO} = 0.87$), as well as to highlight two relevant features for the binding to AM: the presence of a free NH, which is able to establish a hydrogen bond with the receptor, and a phenyl group, which is able to establish hydrophobic interactions. Additional conformational and MD studies have shown the presence of intramolecular bonds in compound **1i** that could compromise this crucial NH group, thus

justifying its behavior as outlier in the 3D-QSAR model and the unexpected low affinity of this compound.

The SAR methodology employed has proved to be a useful tool to elucidate some of the structural requirements to bind AM and to predict affinity. Similar work on negative modulators of AM is in progress in our laboratory.

Experimental Section

Small-Molecule Library. Compounds **1a**−**i** were obtained from the NCI's small-molecule repository. The construction of the library has been described[15] and can be viewed at http://cactus.nci.nih.gov/ncidb2. All compounds were provided diluted in dimethyl sulfoxide (DMSO). NCI codes are 697165 for **1a**, 697161 for **1b**, 697164 for **1c**, 697162 for **1d**, 697163 for **1e**, 697166 for **1f**, 697169 for **1g**, 697167 for **1h**, and 697168 for **1i**.

General Methods. Melting points (uncorrected) were determined on a Stuart Scientific SMP3 apparatus. Infrared (IR) spectra were recorded with a Perkin-Elmer 1330 infrared spectrophotometer. ^{1}H and ^{13}C NMR data were recorded on a Bruker 300-AC instrument. Chemical shifts (δ) are expressed in parts per million relative to internal tetramethylsilane; coupling constants (J) are in hertz. Mass spectra were run on a Bruker Esquire 3000 spectrometer. Elemental analyses (C, H, N) were performed on a Perkin-Elmer 2400 CHN apparatus at the Microanalyses Service of the University Complutense of Madrid. Unless otherwise stated, all reported values are within ±0.4% of the theoretical compositions. Thin-layer chromatography (TLC) was run on Merck silica gel 60 F-254 plates. Unless stated otherwise, starting materials used were high-grade commercial products. Complete ^{1}H and ^{13}C NMR, IR, MS, and elemental analysis data are given in the Supporting Information.

General Procedure for the Preparation of Dihydrazides 2j−**n.** To a stirred suspension of either adipic, pimelic, suberic, azelaic, or sebacic dihydrazide (1 equiv) and phenoxyacetic acid (2 equiv) in CH_3CN was added a solution of $POCl_3$ (8 equiv) in CH_3CN dropwise over 30 min at room temperature. The reaction mixture was heated at reflux temperature until the solution became clear and then for 30 additional minutes. Then, the crude was cooled to room temperature and the solvent was removed under reduced pressure. The obtained residue was poured into ice−water and neutralized with concentrated ammonium. After the mixture was stirred for one night at room temperature, the resulting precipitate was filtered off and recrystallized from absolute EtOH.

***N,N′*-Bis(phenoxyacetyl)adipic Dihydrazide (2j).** From adipic dihydrazide (5.00 g, 28.73 mmol), phenoxyacetic acid (8.73 g, 57.46 mmol), and $POCl_3$ (35.30 g, 229.97 mmol) in CH_3CN (70 mL), **2j** (2.00 g, 16%) was produced as a white solid, mp 237−239 °C (EtOH). IR (KBr): 3420, 3250, 1700, 1660 cm^{-1}. ^{1}H NMR (DMSO-d_6): δ 1.54 (4H, br s, $2CH_2$), 2.50 (4H, br s, $2CH_2CO$), 4.58 (4H, s, $2OCH_2CO$), 6.97 (6H, m, ArH), 7.30 (4H, t, J = 7.9, ArH), 9.83 (2H, s, 2NH), 10.08 (2H, s, 2NH). ^{13}C NMR (DMSO-d_6): δ 24.6, 32.9, 65.9, 114.7, 121.2, 129.4, 157.7, 166.6, 170.9. MS (ESI): m/z 465 $[M + Na]^+$.

***N,N′*-Bis(phenoxyacetyl)pimelic Dihydrazide (2k).** From pimelic dihydrazide (14.53 g, 77.29 mmol), phenoxyacetic acid (23.50 g, 154.60 mmol), and $POCl_3$ (94.90 g, 618.24 mmol) in CH_3CN (180 mL), **2k** (8.10 g, 23%) was produced as a white solid, mp 198−200 °C (EtOH).

***N,N′*-Bis(phenoxyacetyl)suberic Dihydrazide (2l).** From suberic dihydrazide (5.00 g, 24.75 mmol), phenoxyacetic acid (7.52 g, 49.47 mmol), and $POCl_3$ (30.39 g, 197.98 mmol) in CH_3CN (60 mL), **2l** (4.15 g, 36%) was produced as a white solid, mp 202−204 °C (EtOH).

***N,N′*-Bis(phenoxyacetyl)azelaic Dihydrazide (2m).** From azelaic dihydrazide (5.00 g, 23.15 mmol), phenoxyacetic acid (7.03 g, 46.25 mmol), and $POCl_3$ (28.43 g, 185.21 mmol) in CH_3CN (70 mL), **2m** (2.47 g, 23%) was produced as a white solid, mp 172−175 °C (EtOH).

***N,N′*-Bis(phenoxyacetyl)sebacic Dihydrazide (2n).** From sebacic dihydrazide (9.80 g, 42.61 mmol), phenoxyacetic acid (12.95 g, 85.22 mmol), and $POCl_3$ (52.32 g, 340.85 mmol) in CH_3CN (270 mL), **2n** (4.99 g, 25%) was produced as a white solid, mp 188−190 °C (EtOH).

General Procedure for the Preparation of Bisoxadiazoles 3j−**n.** To a stirred suspension of the corresponding dihydrazide (1 equiv) in CH_3CN was added a solution of $POCl_3$ (8 equiv) in CH_3CN dropwise over 30 min at room temperature. The resulting mixture was heated at reflux temperature for 7 h. Then, the crude was cooled to room temperature and the solvent was removed under reduced pressure. The obtained residue was poured into ice−water and neutralized with concentrated ammonium. After the mixture was stirred for one night at room temperature, the resulting precipitate was filtered off and purified by flash column chromatography on sicila gel to give the corresponding oxadiazole.

1,4-Bis(5-phenoxymethyl[1,3,4]oxadiazol-2-yl)butane (3j). From **2j** (2.50 g, 5.66 mmol) and $POCl_3$ (6.95 g, 45.28 mmol) in CH_3CN (35 mL), a white solid was produced. Flash chromatography of the crude product using hexane−AcOEt (1:1) as eluent gave **2j** (1.75 g, 76%), mp 75−78 °C (EtOH). IR (KBr): 1600, 1570 cm^{-1}. ^{1}H NMR ($CDCl_3$): δ 1.93 (4H, br s, $2CH_2$), 2.93 (4H, br s, $2CH_2CNO$), 5.24 (4H, s, $2CH_2O$), 7.02 (6H, m, ArH), 7.31 (4H, m, ArH). ^{13}C NMR ($CDCl_3$): δ 24.9, 25.4, 59.8, 114.8, 122.2, 129.7, 157.5, 162.6, 167.4. MS (ESI): m/z 407 $[M + H]^+$. Anal. ($C_{22}H_{22}N_4O_4$) C, H, N.

1,5-Bis(5-phenoxymethyl[1,3,4]oxadiazol-2-yl)pentane (3k). From **2k** (1.32 g, 2.89 mmol) and $POCl_3$ (3.55 g, 23.13 mmol) in CH_3CN (20 mL), a solid was produced. Flash chromatography of the crude product using CH_2Cl_2−MeOH (99:1) as eluent gave **3k** (716 mg, 59%), mp 71−72 °C (EtOH).

1,6-Bis(5-phenoxymethyl[1,3,4]oxadiazol-2-yl)hexane (3l). From **2l** (3.60 g, 7.66 mmol) and $POCl_3$ (9.40 g, 61.24 mmol) in CH_3CN (50 mL), a white solid was produced. Flash chromatography of the crude product using hexane−AcOEt (1:1) as eluent gave **3l** (920 mg, 28%), mp 57−60 °C (EtOH).

1,7-Bis(5-phenoxymethyl[1,3,4]oxadiazol-2-yl)heptane (3m). From **2m** (2.00 g, 4.13 mmol) and $POCl_3$ (5.07 g, 33.03 mmol) in CH_3CN (25 mL), an oil was produced. Flash chromatography of the crude product using hexane−AcOEt (1:1) as eluent gave **3m** (1.17 g, 63%) as an oil, which crystalized on standing to form a white solid, mp 48−52 °C (EtOH).

1,8-Bis(5-phenoxymethyl[1,3,4]oxadiazol-2-yl)octane (3n). From **2n** (1.30 g, 2.61 mmol) and $POCl_3$ (3.20 g, 20.85 mmol) in CH_3CN (16 mL), a white solid was produced. Flash chromatography of the crude product using toluene−AcOEt (8:2) as eluent gave **3n** (844 mg, 70%), mp 95−99 °C (EtOH).

General Procedure for the Preparation of Bistriazoles 1j−**n.** A mixture of the corresponding bisoxadiazole and an excess of benzylamine was heated at 150 °C for 30 h under argon. The reaction mixture was cooled to room temperature, and CH_2Cl_2 (25 mL) was added. The solution was washed with 10% aqueous HCl, saturated aqueous $NaHCO_3$, and brine. The extract was dried ($MgSO_4$), filtered, and evaporated to dryness, and the obtained crude product was purified by flash column chromatography on silica.

1,4-Bis(4-benzyl-5-phenoxymethyl[1,2,4]triazol-3-yl)-butane (1j). From **3j** (200 mg, 0.49 mmol) and benzylamine (3 mL, 27.48 mmol) and after flash chromatography of the crude product using $CHCl_3$−MeOH (95:5) as eluent, **1j** (84 mg, 30%) was produced as a white solid, mp 190−192 °C (EtOH). IR (KBr): 1600, 1590 cm^{-1}. ^{1}H NMR ($CDCl_3$): δ 1.72 (4H, br s, $2CH_2$), 2.53 (4H, br s, $2CH_2CN_2$), 5.08 (4H, s, $2CH_2N$), 5.13 (4H, s, $2CH_2O$), 6.86 (10H, m, ArH), 7.20 (10H, m, ArH). ^{13}C NMR ($CDCl_3$): δ 24.5, 26.1, 47.0, 60.6, 114.6, 121.8, 126.3, 128.3, 129.1, 129.6, 134.6, 150.8, 155.9, 157.5. MS (ESI): m/z 585 $[M + H]^+$. Anal. ($C_{36}H_{36}N_6O_2$) C, H, N.

1,5-Bis(4-benzyl-5-phenoxymethyl[1,2,4]triazol-3-yl)-pentane (1k). From **3k** (100 mg, 0.24 mmol) and benzylamine (1 mL, 9.16 mmol) and after flash chromatography of the crude product using $CHCl_3$−MeOH (94:6) as eluent, **1k** (31 mg, 22%) was produced as a white solid, mp 94−97 °C (EtOH).

1,6-Bis(4-benzyl-5-phenoxymethyl[1,2,4]triazol-3-yl)-hexane (1l). From **3l** (620 mg, 1.43 mmol) and benzylamine (2 mL, 18.32 mmol) and after flash chromatography of the crude product using $CHCl_3$−MeOH (98:2) as eluent, **1l** (236 mg, 27%) was produced as a white solid, mp 145−147 °C (EtOH).

1,7-Bis(4-benzyl-5-phenoxymethyl[1,2,4]triazol-3-yl)-heptane (1m). From **3m** (300 mg, 0.67 mmol) and benzylamine (1.5 mL, 13.74 mmol) and after flash chromatography of the crude product using $CHCl_3$/MeOH (98:2) as eluent, **1m** (214 mg, 51%) was produced as a white solid, mp 92−94 °C (EtOH).

1,8-Bis(4-benzyl-5-phenoxymethyl[1,2,4]triazol-3-yl)octane (1n). From **3n** (315 mg, 0.68 mmol) and benzylamine (1 mL, 9.16 mmol) and after flash chromatography of the crude product using $CHCl_3$/MeOH (98:2) as eluent, **1n** (179 mg, 42%) was produced as a white solid, mp 109−111 °C (EtOH).

Biological Activity. Synthetic human AM was purchased from Peninsula (S. Carlos, CA). Neutralizing monoclonal antibody against AM was produced by Cuttitta et al.[16,17] and labeled with peroxidase using EZ-Link plus activated peroxidase (Pierce, Rockford, IL).

Human AM was attached to PVC 96-well plates by passive absorption that involved incubating 50 μL of AM (at 1 ng/μL) in 50 μL of phosphate buffer saline (PBS) per well for 1 h. After the coating solution was discarded, wells were washed with 200 μL of PBS three times. Immediately after, an amount of 200 μL of 1% BSA in PBS was added and the solution was incubated for 1 h. Then, this solution was aspirated off and 50 μL containing 1 μM of one of the compounds **1j**−**n**, **2j**−**n**, or **3j**−**n** in 1% bovine serum albumin (BSA)−0.1% Tween-20 in PBS was added. After 1 h, 50 μL of peroxidase-labeled antibody (at 2.4 μg/mL) were added and the solution was allowed to react for 1 h. Following three thorough washes with 200 μL of 1% BSA in PBS, peroxidase activity was developed using *o*-phenylenediamine dihydrochloride (Sigma) as a substrate. The reaction product was quantified with a plate reader (ASYS HiTech Expert 96) at 450 nm. Each plate contained several internal controls including wells without any coating that are used to calculate nonspecific binding, wells where no potential modulators were added, which provided maximum binding, and wells where the unlabeled antibody (at 1.2 μg/mL) substituted the small molecule, as a positive inhibition control. Each compound was added to triplicate wells in the same plate. A positive hit was defined as a compound able to significantly reduce the amount of product in three independent plates. The intraassay variation was 6%, and the interassay variation was 13%. The sensitivity of the assay, as calculated with the cold antibody, was 12 nM, and the dynamic range was between 12 and 54 nM.

3D-QSAR Analysis. The 3D geometries for the compounds of the series were obtained automatically from their structures in the SMILES format using the program CORINA.[18] This method produces reasonable extended conformations for all the compounds, which is appropriate for the QSAR analysis of congeneric series, as the present one. The conformations obtained from CORINA[18] were then analyzed using the grid-independent descriptors (GRIND) methodology with the program ALMOND 3.2,[11] which contains version 19 of the program GRID. DRY, N1, and O probes were chosen in order to represent potentially important groups of the binding site. Molecular shape field (TIP "probe") was also included.[19] This descriptor characterizes the convexity of the molecule, which can indicate the position and spatial extent of chemical groups and of the molecule as a whole. The structures and affinities (*y* variable) of the AM agonists are presented in Table 1. The ALMOND parameters were set to default, the ALMD directive was equal to 1, and the size of the correlograms was automatically established by the program. The baseline was removed for scaling. Cross-validation was done by using the leave-one-out (LOO) method or by assigning the compounds randomly to five groups, performing cross-validation on these groups, and then repeating the whole procedure 20 times. No relevant differences were found between both validation methods. All computations were carried out on an Intel Pentium 4 using the Linux RedHat 9 operating system.

Conformational Analysis. Conformational studies were performed using Macromodel 7.2. The MMFF94s[20] force field was used in combination with the GB/SA solvation model.[21] The model includes both generalized Born based (GB) solvent polarization terms and surface area based (SA) terms.[22,23] Default values were set for the nonbonded interactions cutoff. Energy minimizations were performed with the Powell−Reeves conjugated gradient (PRCG),[24] and the derivate convergence criterion was set to 1.0 kJ Å^{-1} mol^{-1}. Conformational search was performed by the Monte Carlo method[25] for the random variation of all of the rotable bonds combined with the so-called low mode conformational search (LMCS) algorithm.[26] For each calculation 1000 Monte Carlo steps were carried out followed by 500 minimization iterations.

Molecular Dynamics of Compounds 1h and 1i. Molecular dynamics were performed using AMBER.[14] Highly accurate evaluations of the atomic point charges were carried out by means of quantum chemical calculations at the HF/6-31G* level of theory using Gaussian 98[27] followed by the RESP fitting procedure.[28] Additional force field parameters of compounds **1h** and **1i** are given in the Supporting Information. All the simulations were carried out in the presence of solvent (water box size = 35 Å^3). After minimization and 30 ps of equilibration dynamics, the compounds were submitted to a 500 ps restricted dynamics simulation (from 20 to 0 kcal mol^{-1} along 500 ps) on those atoms that were able to establish hydrogen bonds in the conformational search performed earlier. Finally, 1 ns of unrestricted dynamics simulation was performed for all the compounds.

Acknowledgment. This work was supported by the Universidad San Pablo-CEU (Grant No. 5/02). S.M.-S. thanks Ministerio de Educación y Ciencia for a Ramón y Cajal contract. A grant to M.A.G. from Fundación Universitaria San Pablo CEU is also acknowledged. A.M. is supported by a grant from the Ministerio de Educación y Ciencia (Grant BFU 2004-02838/BFI).

Supporting Information Available: ^{1}H and ^{13}C NMR, IR, and MS data of compounds **2k**−**n**, **3k**−**n**, and **1k**−**n**, additional force field parameters of compounds **1h** and **1i**, and microanalysis data for compounds **1j**−**n** and **3j**−**n**. This material is available free of charge via the Internet at http://pubs.acs.org.

References

(1) Martínez, A.; Julián, M.; Bregonzio, C.; Notari, L.; Moody, T.; et al. Identification of vasoactive non-peptidic positive and negative modulators of adrenomedullin using a neutralizing antibody-based screening strategy. *Endocrinology* **2004**, *145*, 3858−3865.

(2) Kitamura, K.; Kangawa, K.; Kawamoto, M.; Ichiki, Y.; Nakamura, S.; et al. Adrenomedullin: a novel hypotensive peptide isolated from human pheochromocytoma. *Biochem. Biophys. Res. Commun.* **1993**, *192*, 553−560.

(3) Hinson, J. P.; Kapas, S.; Smith, D. M. Adrenomedullin, a multifunctional regulatory peptide. *Endocr. Rev.* **2000**, *21*, 138−167.

(4) López, J.; Martínez, A. Cell and molecular biology of the multifunctional peptide, adrenomedullin. *Int. Rev. Cytol.* **2002**, *221*, 1−92.

(5) Julián, M.; Cacho, M.; García, M. A.; Martín-Santamaría, S.; de Pascual-Teresa, B.; Ramos, A.; et al. Adrenomedullin: a new target for the design of small molecule modulators with promising pharmacological activities. *Eur. J. Med. Chem.*, in press.

(6) Dobrzynski, E.; Wang, C.; Chao, J.; Chao, L. Adrenomedullin gene delivery attenuates hypertension, cardiac remodeling, and renal injury in deoxycorticosterone acetate-salt hypertensive rats. *Hypertension* **2000**, *36*, 995−1001.

(7) Martínez, A.; Vos, M.; Guedez, L.; Kaur, G.; Chen, Z.; et al. The effects of adrenomedullin overexpresion in breast tumor cells. *J. Natl. Cancer Inst.* **2002**, *94*, 1226−1237.

(8) Martínez, A.; Elsasser, T. H.; Bhathena, S. J.; Pío, R.; Buchanan, T. A.; et al. Is adrenomedullin a causal agent in some cases of type 2 diabetes? *Peptides* **1999**, *20*, 1471−1478.

(9) Kudari, S. M.; Badiger, S. E. Synthesis of new series of 1,8-bis-(5-aroloxy substituted 1,3,4-oxadiazol-2-yl)octanes, 1,8-bis(5-aroloxy substituted 4-amino/anilino 1,2,4-triazol-2-yl)octanes. *Orient. J. Chem.* **1997**, *13*, 245−248.
(10) Goodford, P. J. A computational procedure for determining energetically favorable binding sites on biologically important macromolecules. *J. Med. Chem.* **1985**, *28*, 849−857.
(11) *ALMOND*, version 3.2; Molecular Discovery Ltd. (215 Marsh Road, Pinner, Middlesex, U.K.), 2004.
(12) Pastor, M.; Cruciani, G.; McLay, I.; Pickett, S.; Clementi, S. GRid-INdependent Descriptors (GRIND): a novel class of alignment-independent three-dimensional molecular descriptors. *J. Med. Chem.* **2000**, *43*, 3233−3243.
(13) Mohamadi, F.; Richards, N. G. J.; Guida, W. C.; Liskamp, R.; Lipton, M.; et al. MacroModel—An integrated software system for modeling organic and bioorganic molecules using molecular mechanics. *J. Comput. Chem.* **1990**, *11*, 440−467.
(14) Case, D. A.; Pearlman, D. A.; Caldwell, J. W.; Cheatham, T. E. I.; Ross, W. S.; et al. *AMBER*, version 6; University of California at San Francisco: San Francisco, CA 1999.
(15) Voigt, J. H.; Bienfait, B.; Wang, S.; Nicklaus, M. C. Comparison of the NCI open database with seven large chemical structural databases. *J. Chem. Inf. Comput. Sci.* **2001**, *41*, 702−712.
(16) Martínez, A.; Weaver, C.; López, J.; Bhathena, S. J.; Elsasser, T. H.; et al. Regulation of insulin secretion and blood glucose metabolism by adrenomedullin. *Endocrinology* **1996**, *137*, 2626−2632.
(17) Cuttitta, F.; Carney, D. N.; Mulshine, J.; Moody, T. W.; Fedorko, J.; et al. Bombesin-like peptides can function as autocrine growth factors in human small-cell lung cancer. *Nature* **1985**, *316*, 823−826.
(18) Gasteiger, J.; Rudolph, C.; Sadowski, J. Automatic generation of 3D atomic coordinates for organic molecules. *Tetrahedron Comput. Methodol.* **1991**, *202*, 537−547.
(19) Fontaine, F.; Pastor, M.; Sanz, F. Incorporating Molecular Shape into the Alignment-Free Grid-Independent Descriptors. *J. Med. Chem.* **2004**, *47*, 2805−2815.
(20) Halgren, T. A. MMFF VII. Characterization of MMFF94, MMFF94s, and other widely available force fields for conformational energies and for intermolecular-interaction energies and geometries. *J. Comput. Chem.* **1999**, *20*, 730−748.
(21) Still, W. C.; Tempczyk, A.; Hawley, R. C.; Hendrickson, T. Semianalytical treatment of solvation for molecular mechanics and dynamics. *J. Am. Chem. Soc.* **1990**, *112*, 6127−6129.
(22) Weiser, J.; Shenkin, P. S.; Still, W. C. Approximate atomic surface from linear combinations of pairwise overlaps (LCPO). *J. Comput. Chem.* **1999**, *20*, 217−230.
(23) Weiser, J.; Shenkin, P. S.; Still, W. C. Fast, Approximate algorithm for detection of solvent-inaccessible atoms. *J. Comput. Chem.* **1999**, *20*, 586−596.
(24) Polak, E.; Ribiere, G. Note sur la Convergence de Methodes de Directions Conjuguees, Serie Rouge (Note on convergence of conjugated direction methods). *Rev. Fr. Inf. Rech. Oper.* **1969**, *16-R1*.
(25) Chang, G.; Guida, W. C.; Still, W. C. An internal coordinate Monte Carlo method for searching conformational space. *J. Am. Chem. Soc.* **1989**, *111*, 4379−4386.
(26) Kolossvary, I.; Guida, W. C. Low mode search. An efficient, automated computational method for conformational analysis: Application to cyclic and acyclic alkanes and cyclic peptides. *J. Am. Chem. Soc.* **1996**, *118*, 5011−5019.
(27) Frisch, M. J.; Trucks, G. W.; Schlegel, H. B.; Scuseria, G. E.; Robb, M. A.; Cheeseman, J. R.; Zakrzewski, V. G.; Montgomery, J. A., Jr.; Stratmann, R. E.; Burant, J. C.; Dapprich, S.; Millam, J. M.; Daniels, A. D.; Kudin, K. N.; Strain, M. C.; Farkas, O.; Tomasi, J.; Barone, V.; Cossi, M.; Cammi, R.; Mennucci, B.; Pomelli, C.; Adamo, C.; Clifford, S.; Ochterski, J.; Petersson, G. A.; Ayala, P. Y.; Cui, Q.; Morokuma, K.; Malick, D. K.; Rabuck, A. D.; Raghavachari, K.; Foresman, J. B.; Cioslowski, J.; Ortiz, J. V.; Stefanov, B. B.; Liu, G.; Liashenko, A.; Piskorz, P.; Komaromi, I.; Gomperts, R.; Martin, R. L.; Fox, D. J.; Keith, T.; Al-Laham, M. A.; Peng, C. Y.; Nanayakkara, A.; Gonzalez, C.; Challacombe, M.; Gill, P. M. W.; Johnson, B. G.; Chen, W.; Wong, M. W.; Andres, J. L.; Head-Gordon, M.; Replogle, E. S.; Pople, J. A. *Gaussian 98*, revision A.7; Gaussian, Inc.: Pittsburgh, PA, 1998.
(28) Bayly, C. I.; Cieplak, P.; Cornell, W.; Kollman, P. A. A well-behaved electrostatic potential based method using charge restraints for deriving atomic charges: the RESP model. *J. Phys. Chem.* **1993**, *97*, 10269−10280.

JM050021+